Check for updates

Original Research Article

Antithrombic Mechanisms of Viper Venom Platelet Inhibitory Factor in the Rat Myocardial Ischemia-Reperfusion Injury Model

Pharmacognosy Magazine
22(2) 640–650, 2026
© The Author(s) 2025
Article reuse guidelines:
in.sagepub.com/journals-permissions-india
DOI: 10.1177/09731296251340845
journals.sagepub.com/home/phm

Juan Wu[1], Gui-lin Feng[2,3], Wei Li[1], Xue Zhao[1], Neng-sheng Bao[1], Tian-yu Ge[4], Xi Huang[5], Qing-quan Xue[2] and He Zhang[6]

Abstract

Background: Myocardial ischemia-reperfusion injury (MIRI) exacerbates thrombosis and platelet hyperactivation post-revascularization, with limited therapeutic efficacy of existing antiplatelet agents. Agkistrodon halys venom platelet inhibitor (AHVPI) shows uncharacterized antithrombotic potential. This study evaluates AHVPI's mechanistic regulation of key platelet biomarkers and hemostatic parameters in a rat MIRI model.
Objectives: To explore the antithrombic mechanisms of AHVPI in a rat model of MIRI.
Materials and Methods: Thirty male Sprague-Dawley rats were randomized to the sham operation (n = 6), MIRI (n = 6), and AHVPI groups (n = 18). The left anterior descending coronary artery was ligated to form the MIRI model. The AHVPI group included three subgroups (low-dose, medium-dose, and high-dose groups), which were sublingually administered AHVPI at doses of 0.05, 0.1, and 0.2 mg/kg body weight, respectively (six rats per subgroup). Electrocardiographic changes were monitored via the RM6240 biological signal acquisition system. An enzyme-linked immunosorbent assay was used to measure the plasma levels of platelet membrane glycoprotein VI (GPVI) and P-selectin. Thromboelastography (TEG® 5000) was used to assess the clot formation time (K), coagulation time (R), α angle (A), and maximum amplitude (MA) in the rat blood. Whole-blood and plasma viscosity was measured using a cone-plate viscometer, whereas turbidimetry was used to determine the platelet aggregation rate.
Results: Compared with those in the MIRI group, A and MA values ($p < .05$), blood viscosity, aggregation amplitude, platelet aggregation rate ($p < .05$), and the GPVI and P-selectin expression levels ($p < .05$) were prominently lower, and both the K and R values were markedly greater in the medium-dose and high-dose AHVPI groups.
Conclusion: AHVPI considerably inhibits platelet activity, alleviates MIRI-associated hemorheological properties, and mitigates the adverse effects of MIRI in the MIRI rat model.

Keywords

Agkistrodon halys venom platelet inhibitor, antithrombic mechanisms, myocardial ischemia-reperfusion injury, platelet activity, rat model

Received 29 October 2024; **revised** 08 February 2025; **accepted** 14 March 2025

Introduction

Myocardial ischemia-reperfusion injury (MIRI) is an intricate procedure that occurs when ischemic myocardial tissue is reperfused with blood flow, leading to arrhythmias, myocardial stunning, and microvascular dysfunction (Wang, Liu,

Juan Wu and Gui-lin Feng contributed equally to this work.
[1]Department of Pathophysiology, Wannan Medical College, Wuhu, Anhui, China
[2]Department of Vascular Surgery, Yijishan Hospital, The First Affiliated Hospital of Wannan Medical College, Wuhu, Anhui, China.
[3]Department of Vascular Surgery, Tianjin Medical University General Hospital, Tianjin, China
[4]Department of Functional Science Laboratory and Training Center, Wannan Medical College, Wuhu, Anhui, China
[5]Department of Pathology, Yijishan Hospital, The First Affiliated Hospital of Wannan Medical College, Wuhu, Anhui, China
[6]Department of Respiratory and Critical Care Medicine, Yijishan Hospital, The First Affiliated Hospital of Wannan Medical College, Wuhu, Anhui, China

Corresponding authors:
Qing-quan Xue, Department of Vascular Surgery, Yijishan Hospital, The First Affiliated Hospital of Wannan Medical College, No. 2, Zhe Shan Xi Lu Road, Jinghu District, Wuhu, Anhui 241001, China.
E-mail: xueqingqingq@hotmail.com
He Zhang, Department of Respiratory and Critical Care Medicine, Yijishan Hospital, The First Affiliated Hospital of Wannan Medical College, No. 2, Zhe Shan Xi Lu Road, Jinghu District, Wuhu, Anhui 241001, China.
E-mail: zhanghe273654@outlook.com

Creative Commons Non Commercial CC BY-NC: This article is distributed under the terms of the Creative Commons Attribution-NonCommercial 4.0 License (http://www.creativecommons.org/licenses/by-nc/4.0/) which permits non-Commercial use, reproduction and distribution of the work without further permission provided the original work is attributed as specified on the SAGE and Open Access pages (https://us.sagepub.com/en-us/nam/open-access-at-sage).

Liu, et al., 2023; Xing et al., 2022). The no-reflow phenomenon, which is an aberrant condition in which the ischemic area does not achieve adequate reperfusion despite the restoration of blood flow, is one of the manifestations of ischemia-reperfusion injury (IRI). The no-reflow phenomenon occurs closely related to endothelial cell damage, hemorheological alterations, and changes in blood properties. In particular, platelet activation, followed by adhesion, aggregation, and release responses, are key factors regulating the no-reflow phenomenon (Aggarwal et al., 2021; Caiazzo et al., 2020). Therefore, antiplatelet therapy is a key therapeutic regimen for the treatment and prevention of thrombotic cardiovascular and cerebrovascular diseases, as well as for mitigating MIRI (Alpert, 2023; Schanze et al., 2023; Stewart et al., 2019).

Platelet membrane glycoproteins (GPs) mediate platelet adhesion and aggregation, playing a critical role in the initial hemostatic response, the adhesion of platelets with the extracellular matrix, as well as the aggregation of platelets. The molecular structure, type, content, distribution, and function of activated GPs are highly different from those of resting, non-activated GPs. These molecular markers can be used to predict ischemic incidence and evaluate the efficacy of therapies pointed at averting reperfusion injury (Schirone et al., 2022; Schlesinger, 2018).

Agkistrodon halys venom platelet inhibitor (AHVPI) is an active protein isolated and purified from the crude venom of the natural *A. halys* from southern Anhui Province, China. The molecular weight of AHVPI is 31.0 kDa. Previous studies have demonstrated that AHVPI potently inhibits platelet aggregation and fibrinolysis (Huang et al., 2012; Na et al., 2014). In this study, a model of MIRI in rats was constructed through a surgical ligature method to bind the left anterior descending coronary artery (LAD). We aimed to explore the effects of AHVPI on platelet activity and hemorheological properties and elucidate the underlying mechanisms. The findings of this study will provide direct scientific evidence for future clinical application studies.

Materials and Methods

Drugs and Reagents

AHVPI, a potent protein isolated from pit viper venom, was provided by the Snake Venom Research Institute of Wannan Medical College. The following reagents were obtained from different vendors: adenosine diphosphate (ADP) (Sigma, USA), phosphate-buffered saline (Beyotime Biotechnology, China), P-selectin ELISA kit (SolarBio Life Sciences, Shanghai, China), and GPVI ELISA kit (Bioss Biotechnology, Beijing, China).

Instruments

The following instruments were used in this study: Biological signal acquisition and processing system (RM6240, Chengdu Instrument Factory), thromboelastograph (TEG® 5000, Haemoscope, USA), platelet aggregometer (PA100, Chongqing Tianhai Medical Equipment Co., Ltd.), BECKMAN centrifuge (Beckman, USA), microplate reader (Model 680, Bio-Rad, USA), and inverted phase contrast microscope (IX51, Olympus, Japan).

MIRI Rat Model Establishment and Drug Treatment

In accordance with the methods described in previous studies (Fu et al., 2019; Kim et al., 2012; Tong et al., 2022), the rats were anesthetized via the intraperitoneal injection of 0.2 mL/100 g body weight of 1.5% pentobarbital sodium and immobilized. After the RM6240 biological signal acquisition system was set up, needle electrodes were subcutaneously inserted into the ankles of the rats. To record the electrocardiogram (ECG), electrodes were connected to the ECG leads as follows: right forelimb (green), right hindlimb (black), and left forelimb (red). A cervical incision was introduced to insert an endotracheal tube for mechanical ventilation. Access to the thoracic cavity of rats was achieved through the incision made on the left of the fourth intercostal space. Next, the pericardium was cut open to expose the myocardium. A circular non-invasive suture (6/0) was located 2 mm below the beginning of the LAD. After the artery was ligated for 45 min, it was released, and reperfusion was performed for 120 min. The MIRI model was successfully established when the ST segment of the ECG II lead exhibited an elevation of 0.1 mV. Thirty healthy male Sprague-Dawley rats (aged 8–9 weeks; body weight: 200–250 g) were purchased from Nanjing Pengsheng Biotechnology Co., Ltd. (License No.: SC-358791). All the rats were equally and randomly divided into five groups: the sham operation group (control), in which the left coronary artery was punctured but not ligated; the MIRI group, in which the left coronary artery was punctured and ligated; the low-dose AHVPI (AHVPI-low) group, in which the rats were administered AHVPI at a dose of 0.05 mg/kg body weight before MIRI modeling; the medium-dose AHVPI (AHVPI-medium) group, in which the rats were administered AHVPI at 0.1 mg/kg body weight before MIRI modeling; and the high-dose AHVPI (AHVPI-high) group, in which the rats were administered AHVPI at 0.2 mg/kg body weight before MIRI modeling. The number of rats in each experimental group was six during both the model development and study period. All animal experiments were reviewed and approved by the Institutional Animal Ethics Committee of Wannan Medical College (IAEC Protocol Approval Number: Wannan Medical College/IAEC/LLSC-2022-267; approval date: January 20, 2022).

Sample Collection and Measurement of Indicators

Blood samples (8 mL per rat) from the carotid artery of all the rats were collected and well preserved in centrifuge tubes

containing an anticoagulant (3.8% sodium citrate). The expression levels of platelet membrane GPVI and P-selectin in the rats were measured using enzyme-linked immunosorbent assay (ELISA). A cone-plate viscometer was used to determine the high-shear, medium-shear, and low-shear viscosities of whole blood samples, as well as plasma viscosity. Platelet-rich plasma was separated via centrifugation at 1,000 *g* for 10 min. Meanwhile, platelet-poor plasma was acquired via further centrifugation at 3,000 *g* for 10 min. Aggregation of platelets was induced using ADP (20 μL, 10 μmol/L) and measured using turbidimetry to determine the aggregation rates at 1 min (A1), 3 min (A3), and 5 min (A5), and the aggregation amplitude (Song et al., 2005). Thromboelastography was performed to measure clot formation time (*K*), clotting time (*R*), *α* angle (*A*), and maximum amplitude (MA) with kaolin (a type of clay) as the activator (Whitton & Healy, 2023). The content of P-selectin was also measured using a double-antibody sandwich ELISA. At the conclusion of the experiment, cardiac tissues from each group of rats were harvested and fixed in 10% neutral buffered formalin overnight. The tissues were subsequently dehydrated, embedded in paraffin, and sectioned into 5 μm thick slices for hematoxylin and eosin (HE) staining. Following staining, the myocardial tissue sections were examined under a light microscope at 200× magnification, and pathological morphological analysis was conducted.

Statistical Analysis

Normally distributed data were indicated by mean ± standard deviation ($\bar{x} \pm s$). Means across different groups were examined using a one-way analysis of variance and the Student–Newman–Keuls (SNK-q) test. Statistical analyses were calculated by SPSS (version 20.0), and a *p* value of less than .05 was considered significant.

Results

Effects of AHVPI on Blood Viscosity in Rats

The low-shear, medium-shear, and high-shear viscosities of whole blood and plasma viscosity in the control group were far less than those of the MIRI group ($p < .05$). Compared with those in the MIRI group, the low-shear, medium-shear, and high-shear viscosities of whole blood and plasma viscosity were also remarkably lower in the AHVPI-medium and AHVPI-high groups ($p < .05$), but in the control group, there were no significant differences ($p > .05$). The AHVPI-low and MIRI groups presented no substantial differences in viscosity, as did the AHVPI-medium and AHVPI-high groups ($p > .05$; Table 1 and Figure 1). These results suggest that AHVPI effectively decreased blood viscosity in the MIRI rat model.

Effects of AHVPI on Platelet Aggregation in Rats

Compared with those in the MIRI group, the A1, A3, and A5 values and the aggregation amplitude were much lower in the AHVPI-medium and AHVPI-high groups ($p < .05$). However, these parameters did not differ prominently among the sham operation, AHVPI-medium, and AHVPI-high groups ($p > .05$; see Table 2 and Figure 2). These findings indicate that AHVPI significantly reduces platelet activity in rats.

Effects of AHVPI on GPVI and P-selectin Expression in Plasma of Rats

In comparison to the control group, P-selectin and GPVI levels were considerably increased in the MIRI group ($p < .05$). Moreover, P-selectin and GPVI in the AHVPI-medium and AHVPI-high groups were prominently lower than those in the MIRI group ($p < .05$). Nevertheless, the expression levels of P-selectin and GPVI did not substantially differ among the control, AHVPI-medium, and AHVPI-high groups ($p > .05$; Table 3 and Figure 3).

Effects of AHVPI on Myocardial Tissue in Rats

Histopathological examination of myocardial tissue was performed via HE staining. As shown in Figures 4B and 4C, significant myocardial swelling and nuclear condensation were observed in the MIRI and AHVPI-low groups. In contrast, the sham operation, AHVPI-medium, and AHVPI-high groups presented well-preserved myocardial cell morphology with clear cell boundaries (Figure 4A, 4D, and 4E). Furthermore,

Table 1. Effect of AHVPI on Blood Viscosity in Rats.

Group	*n*	Whole-blood High-shear Viscosity ((150 S^{-1})/mPa s)	Whole-blood Medium-shear Viscosity ((60 S^{-1})/mPa s)	Whole-blood Low-shear Viscosity ((5 S^{-1})/mPa s)	Plasma Viscosity ((100 S^{-1})/mPa s)
Control	6	3.78 ± 0.40*	3.27 ± 0.72*	5.48 ± 0.93*	1.21 ± 0.07*
MIRI	6	5.71 ± 0.53#	6.91 ± 0.93#	9.06 ± 0.80#	1.88 ± 0.06#
AHVPI-low	6	5.58 ± 0.66#	6.78 ± 0.53#	8.78 ± 0.67#	1.76 ± 0.10#
AHVPI-medium	6	4.07 ± 0.56*	4.01 ± 0.62*	6.14 ± 0.65*	1.34 ± 0.13*
AHVPI-high	6	3.89 ± 0.49*	3.69 ± 0.69*	5.83 ± 0.79*	1.29 ± 0.14*

Notes: AHVPI: *Agkistrodon halys* venom platelet inhibitor; MIRI: Myocardial ischemia-reperfusion injury. Superscripts with the same symbol (* or #) indicate a *p* value of more than .05 between groups. A *p* value of less than .05 between groups is indicated by superscripts with different symbols.

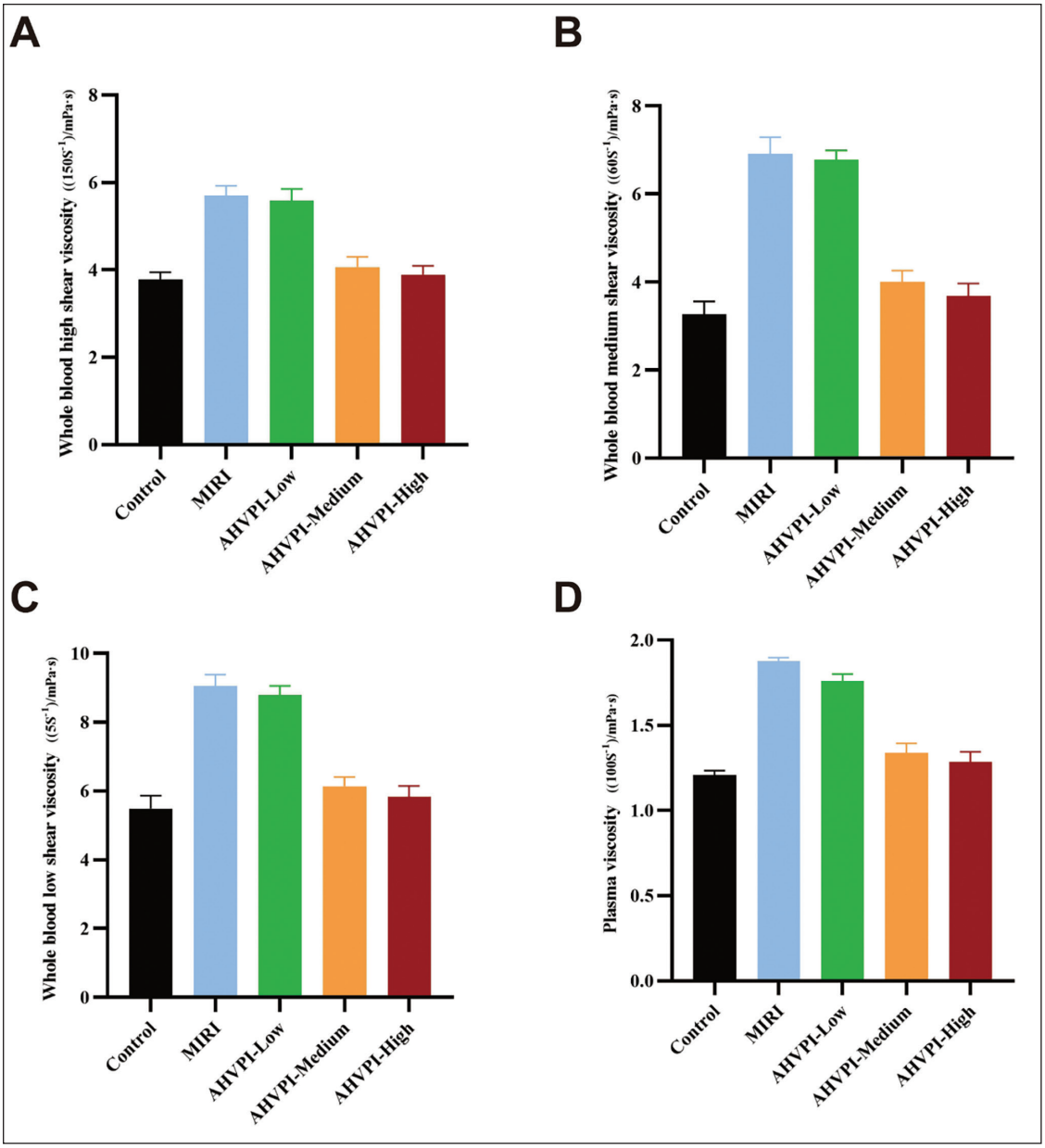


Figure 1. Effects of AHVPI on Blood Viscosity in Rats. (A) Comparison of Whole-blood High-shear Viscosity Among the Different Groups; (B) Comparison of Whole-blood Medium-shear Viscosity Among the Different Groups; (C) Comparison of Whole-blood Low-shear Viscosity Among the Different Groups; (D) Comparison of Plasma Viscosity in Different Groups.

Note: AHVPI: *Agkistrodon halys* venom platelet inhibitor; MIRI: Myocardial ischemia-reperfusion injury.

Table 2. Effect of AHVPI on Platelet Aggregation in Rats.

Group	*n*	A1 (%)	A3 (%)	A5 (%)	Aggregation Amplitude (%)
Control	6	34.33 ± 8.73*	47.83 ± 11.55*	51.50 ± 10.31*	50.50 ± 13.75*
MIRI	6	50.34 ± 10.84#	82.84 ± 8.78#	85.83 ± 6.11#	88.83 ± 5.31#
AHVPI-low	6	50.83 ± 9.52#	83.17 ± 7.63#	88.17 ± 5.53#	89.17 ± 3.97#
AHVPI-medium	6	38.67 ± 5.28*	51.83 ± 6.65*	56.67 ± 10.01*	58.17 ± 12.84*
AHVPI-high	6	36.50 ± 5.40*	49.67 ± 11.06*	53.50 ± 9.40*	55.67 ± 12.71*

Notes: AHVPI: *Agkistrodon halys* venom platelet inhibitor; A1, Aggregation rate of platelets at 1 min; A3: Aggregation rate of platelets at 3 min; A5: Aggregation rate of platelets at 5 min; MIRI: Myocardial ischemia-reperfusion injury. Superscripts with the same symbol (* or #) indicate a *p* value of more than .05 between groups. A *p* value of less than .05 between groups is indicated by superscripts with different symbols.

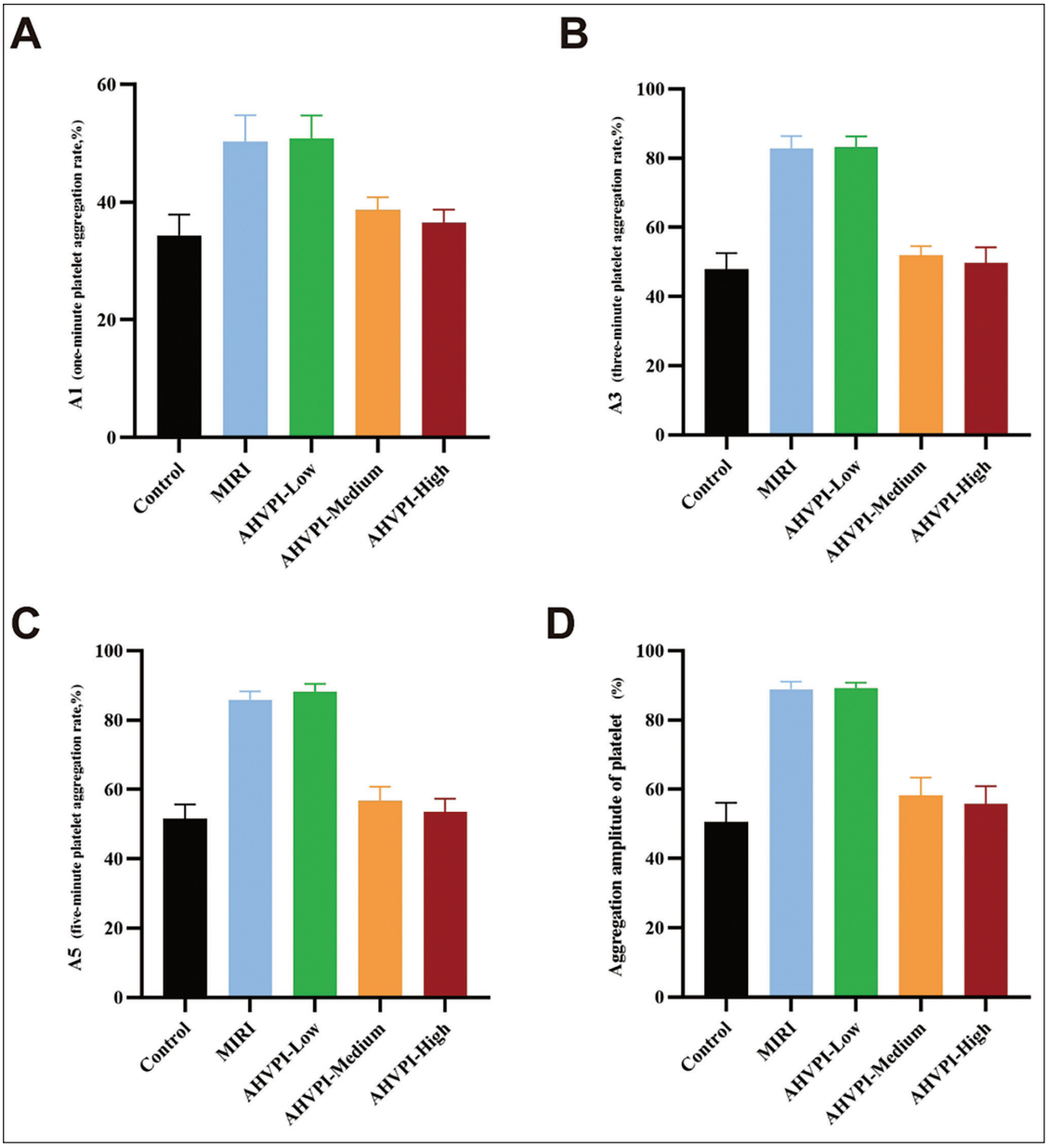


Figure 2. Effects of AHVPI on Platelet Aggregation in Rats. (A) Comparison of Platelet Aggregation at 1 min (A1) in Different Groups; (B) Comparison of Platelet Aggregation at 3 min (A3) in Different Groups; (C) Comparison of Platelet Aggregation at 5 min (A5) in Different Groups; (D) Comparison of Platelet Aggregation Amplitudes in Different Groups.

Note: AHVPI: *Agkistrodon halys* venom platelet inhibitor; MIRI: Myocardial ischemia-reperfusion injury.

Table 3. Expression Levels of GPVI and P-selectin.

Group	*n*	GPVI (ng/mL)	P-selectin (μg/L)
Control	6	1.14 ± 0.32*	1.44 ± 0.21*
MIRI	6	3.35 ± 1.45#	2.32 ± 0.24#
AHVPI-low	6	3.23 ± 1.49#	2.28 ± 0.16#
AHVPI-medium	6	1.92 ± 0.60*	1.74 ± 0.33*
AHVPI-high	6	1.51 ± 0.39*	1.58 ± 0.46*

Notes: AHVPI: *Agkistrodon halys* venom platelet inhibitor; GPVI: Glycoprotein VI; MIRI: Myocardial ischemia-reperfusion injury. Superscripts with the same symbol (* or #) indicate a *p* value of more than .05 between groups. A *p* value of less than .05 between groups is indicated by superscripts with different symbols.

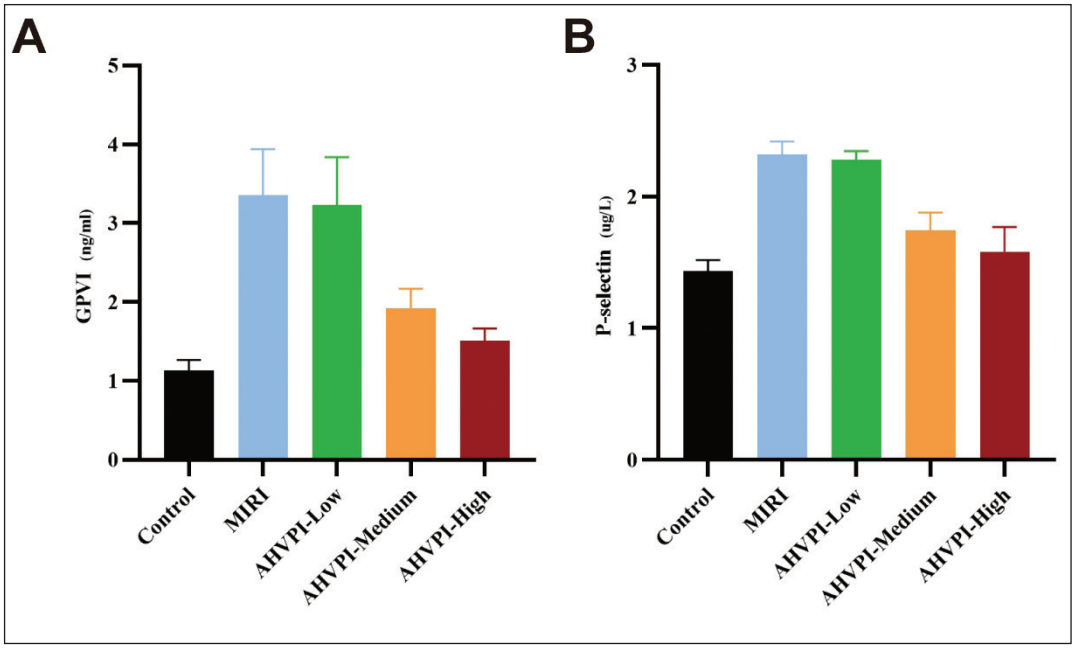


Figure 3. Effects of AHVPI on GPVI and P-selectin Expression in Plasma of Rats. (A) Comparison of GPVI Expression Levels in Different Groups; (B) Comparison of P-selectin Expression Levels in Different Groups.

Note: AHVPI: *Agkistrodon halys* venom platelet inhibitor; GPVI: Glycoprotein VI; MIRI: Myocardial ischemia-reperfusion injury.

the AHVPI-high and AHVPI-medium groups exhibited less pronounced myocardial cell swelling and nuclear condensation compared to the MIRI and AHVPI-low groups, with certain regions showing no significant signs of either.

The Thromboelastograms of Different Rat Groups

In contrast to those in the MIRI and AHVPI-low groups (Figure 5B and 5C), the values of *K* and *R* were markedly greater (Figure 5G and 5F), and the values of MA and *A* were much lower in the AHVPI-medium and AHVPI-high groups (Figure 5I, 5H, 5D, and 5E) ($p < .05$). Thus, treatment with AHVPI at medium and high doses effectively mitigated the enhanced coagulation status in the MIRI model (Figure 5A–5I and Table 4). Additionally, optimal dosing of AHVPI can considerably suppress elevated blood coagulation states.

Discussion

The specific pathophysiological mechanisms underlying IRI have not been elucidated. Although advances in treatment methods for myocardial ischemia have contributed to functional recovery and damage repair of tissues or organs through the restoration of blood flow, ischemia-reperfusion may sometimes exacerbate functional impairment and structural damage instead of restoring organ function. Thus, MIRI is a major challenge for clinicians in treating patients with ischemic heart disease (Sagris et al., 2024). The current consensus in the medical field suggests that MIRI is closely associated with endothelial cell damage, changes in blood properties, and alterations in blood rheology. Additionally, platelet activation plays a significant role in MIRI pathogenesis. Platelets, which are in a quiescent state in the circulation, are activated in response to thrombin, ADP, or contact with damaged endothelial cells and collagen. Platelet activation results in the adhesion, aggregation, and release of platelet procedures, regulating the hemostatic process. Although platelet activation is a physiological response, its dysregulation can contribute to the occurrence and progression of MIRI (Parodi et al., 2011; Wang, Liu, Tian, et al., 2023). Uncontrolled platelet activation or regulatory dysfunction can lead to secondary thrombus formation, resulting in diseases including myocardial infarction or ischemic stroke (Chatterjee et al., 2020; Nieswandt et al., 2011). Previous studies have reported that patients with MIRI exhibit a hypercoagulable state with high proportions and activities of activated platelets. Thus, platelets are major risk factors for MIRI. This study examined the effects of AHVPI on platelet activity in the MIRI rat model. Importantly, pretreatment with appropriate doses of AHVPI improved platelet function, blood properties, and overall state, attenuating the pathological process of MIRI. These findings suggest that AHVPI exerts effective protective effects in the MIRI model, although further studies into its safety profile are warranted.

Platelet membrane GPs, including GPVI, are crucial factors for platelet activation, adhesion, and aggregation, directly influencing platelet status and function (Nuyttens et al., 2011; Yang et al., 2019). Consequently, GPs are considered molecular markers of activated platelets. Clinical studies in acute

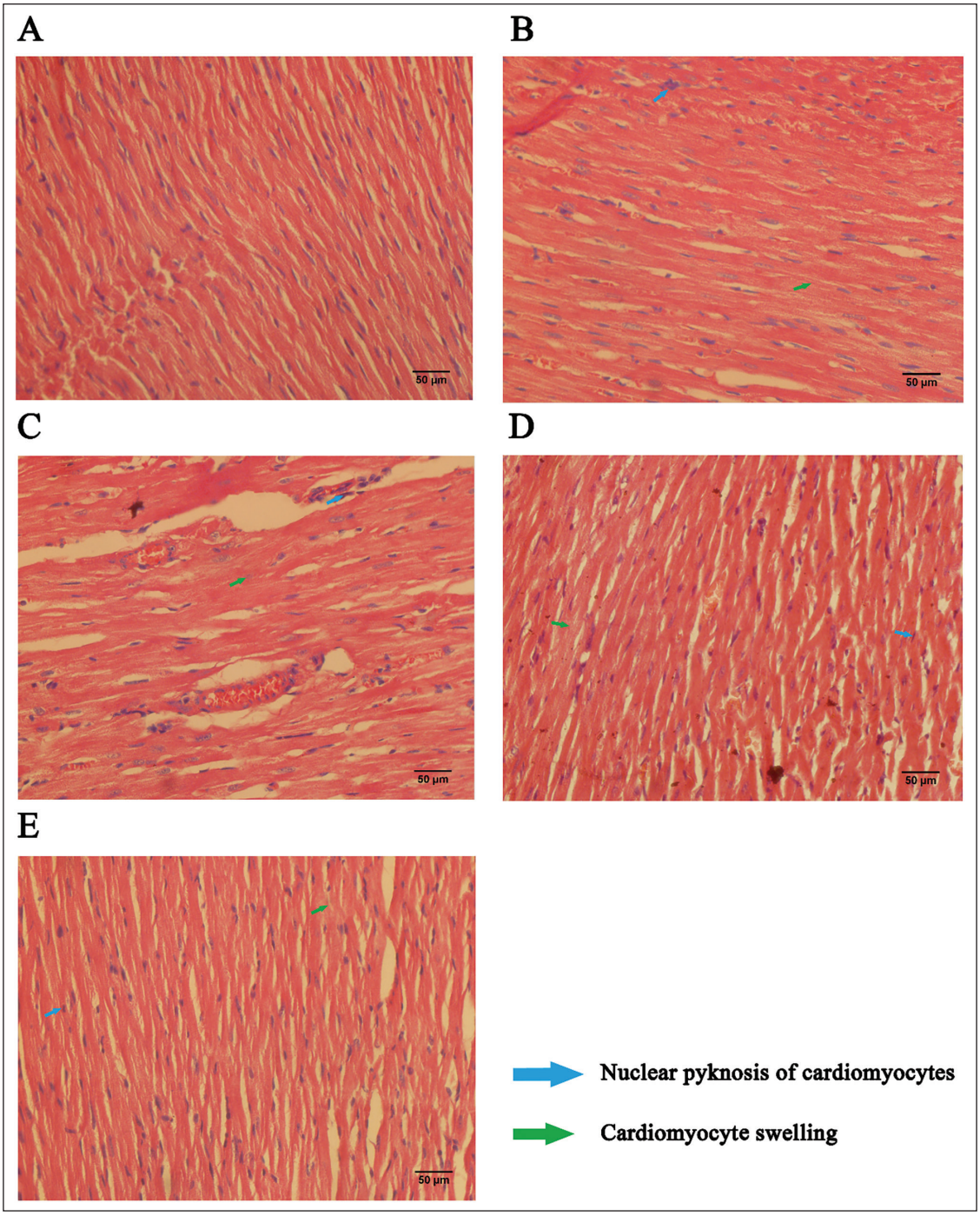


Figure 4. Effects of AHVPI on Myocardial Tissue in Rats. (A) Rat Myocardial Tissue from the Control Group was Stained with HE (Light Microscopy; Magnification ×200); (B) Myocardial Tissue from the MIRI Group was Stained with HE (Light Microscopy; Magnification ×200); (C) Rat Myocardial Tissue from the AHVPI-low Group was Stained with HE (Light Microscopy; Magnification ×200); (D) Rat Myocardial Tissue from the AHVPI-medium Group was Stained with HE (Light Microscopy; Magnification ×200); (E) Rat Myocardial Tissue from the AHVPI-high Group was Stained with HE (Light Microscopy; Magnification ×200).

Note: AHVPI: *Agkistrodon halys* venom platelet inhibitor; AHVPI-high: *Agkistrodon halys* venom platelet inhibitor at a high-dose (0.2 mg/kg body weight); AHVPI-low: *Agkistrodon halys* venom platelet inhibitor at a low-dose (0.05 mg/kg body weight); AHVPI-medium: *Agkistrodon halys* venom platelet inhibitor at a medium dose (0.1 mg/kg body weight); HE: Hematoxylin and eosin; MIRI: Myocardial ischemia-reperfusion injury.

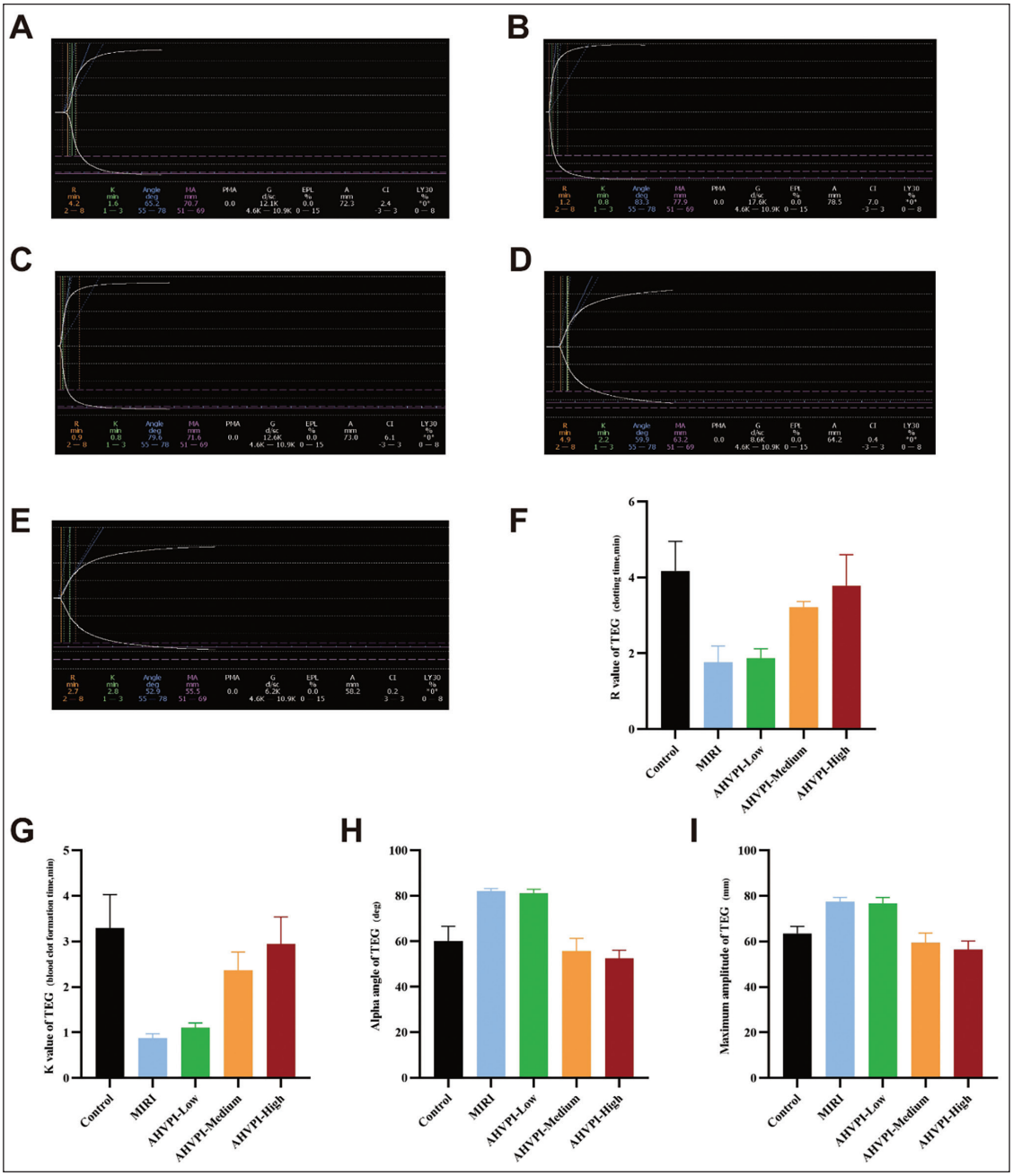


Figure 5. The Thromboelastograms of Different Rat Groups. (A) Thromboelastogram of the Control Group; (B) Thromboelastogram of the MIRI Group; (C) Thromboelastogram of the AHVPI Low-dose (0.05 mg/kg body weight) Group; (D) Thromboelastogram of the AHVPI Medium-dose (0.1 mg/kg body weight) Group; (E) Thromboelastogram of the AHVPI High-dose (0.2 mg/kg body weight) Group; (F) Coagulation Time (*R*) Calculated from Thromboelastogram (TEG); (G) Clot Formation Time (*K*) Calculated from Thromboelastogram (TEG); (H) α Angle (*A*) Calculated from Thromboelastogram (TEG); (I) Maximum Amplitude Calculated from TEG.

Note: AHVPI: *Agkistrodon halys* venom platelet inhibitor; MIRI: Myocardial ischemia-reperfusion injury.

myocardial infarction (AMI) sufferers have revealed that the probability of a lack of myocardial reflow following ischemic myocardial reperfusion therapy is closely related to GP expression levels. Thus, the effect of GPs on thrombosis has piqued clinicians' interest (Senis et al., 2014; Slater et al., 2024). GPVI, a collagen receptor expressed on the membrane of platelets, facilitates platelet activation and adhesion through its interaction with collagen. Prior research has indicated that GPVI expression levels are largely upregulated in various vascular diseases, including cerebral apoplexy and AMI (Gawaz et al., 2014; Zahid et al., 2011). Therefore, GPVI is essential for thrombus formation and development

Table 4. Effects of Viper Venom Platelet Inhibitory Factors on Thromboelastogram Parameters in Rats.

Group	*n*	*R* (min)	*K* (min)	*α* Angle (°)	Maximum Amplitude (mm)
Control	6	4.17 ± 1.90*	3.29 ± 1.81*	60.09 ± 16.13*	63.58 ± 7.45*
MIRI	6	1.76 ± 1.05#	0.88 ± 0.23#	82.13 ± 2.67#	77.54 ± 4.52#
AHVPI-low	6	1.87 ± 0.60#	1.10 ± 0.27#	81.10 ± 4.27#	76.72 ± 6.60#
AHVPI-medium	6	3.22 ± 0.84*	2.37 ± 0.98*	55.74 ± 13.3*	59.44 ± 10.54*
AHVPI-high	6	3.78 ± 2.01*	2.95 ± 1.45*	52.58 ± 8.75*	56.42 ± 9.37*

Notes: AHVPI: *Agkistrodon halys* venom platelet inhibitor; *K*: Clot formation time; MIRI: Myocardial ischemia-reperfusion injury; *R*: Coagulation time. Superscripts with the same symbol (* or #) indicate a *p* value of more than .05 between groups. A *p* value of less than .05 between groups is indicated by superscripts with different symbols.

(Borst & Gawaz, 2021). In view of this, elucidation of the micro-effect on platelet activation induced by GPVI is a major research focus (Stoll et al., 2024). Rat studies have demonstrated that the exposure of endothelial cells and subendothelial tissues resulting from tissue damage impairs platelet aggregation due to the absence or inactivation of GPVI. Furthermore, other important surface receptors of the platelet membrane, for instance, GPIb-V-IX, cannot promote platelet aggregation and adhesion in the absence of active GPVI (Schulz et al., 2010). These findings confirm the vital importance of GPVI in both platelet activation and subsequent thrombosis. Our results indicate that optimal AHVPI pretreatment significantly downregulates GPVI expression in MIRI rats, attenuating GPVI-driven platelet activity and improving blood viscosity and hemorheology. This pathway may be one of the key mechanisms underlying the protective effects of AHVPI against MIRI. Notably, our findings align with previous studies demonstrating the critical role of GPVI in platelet activation and thrombosis during IRI (Veninga et al., 2022). For instance, GPVI has been shown to mediate collagen-induced platelet aggregation and thrombus formation, which are central to the pathogenesis of MIRI (Fuentes, 2022). However, unlike earlier research focusing on GPVI inhibition through pharmacological agents or genetic modifications, our study highlights the unique ability of AHVPI, a natural protein derived from pit viper venom, to modulate GPVI expression and function. This novel approach not only provides a potential therapeutic strategy for MIRI but also offers new insights into the regulation of platelet-related pathways in cardiovascular diseases (Navarro et al., 2022).

P-selectin, also known as CD62P, is predominantly found in Weibel–Palade bodies from vascular endothelial cells or in the membranes of alpha-granules within platelets. Upon platelet activation, CD62P is exposed to the surface of the platelet membrane and partially released into the bloodstream (Denorme & Campbell, 2022). The expression level of CD62P in the blood is significantly increased during IRI. Furthermore, CD62P expression is positively correlated with thrombotic events by enhancing platelet activation and thrombus formation (Alenazy & Thomas, 2021; McEver, 2015). In contrast, our findings demonstrate that AHVPI effectively suppresses P-selectin expression, thereby disrupting the pathological cascade of platelet activation and leukocyte-endothelial interactions. This mechanism is consistent with previous studies showing that modulation of P-selectin can attenuate IRI-induced tissue damage (Farmer et al., 2005). In addition to its effects on P-selectin, AHVPI may also target other platelet receptors, such as GPVI, which play a critical role in platelet adhesion and aggregation. This multi-target approach may enhance the therapeutic efficacy of AHVPI by simultaneously addressing multiple aspects of platelet dysfunction and endothelial activation, thereby offering a more comprehensive strategy for mitigating MIRI.

Conclusion

In summary, this study demonstrates that AHVPI effectively downregulated the expression of platelet activation markers, GPVI and CD62P, in a rat model of MIRI. At optimal doses, the robust efficacy of AHVPI in suppressing platelet activation and alleviating myocardial injury establishes an experimental foundation for its further development as a clinical therapeutic for MIRI. However, two limitations should be noted: (a) whether AHVPI modulates GPVI/CD62P expression via GPVI-dependent signaling cascades requires further mechanistic investigation; (b) dynamic alterations in ejection fraction, fractional shortening, and MIRI lesion area across AHVPI-treated groups were not comprehensively assessed. If approved for further research, we will integrate cardiac function monitoring, molecular mechanism elucidation, and safety assessment to advance the clinical translation of AHVPI and the development of novel antithrombotic agents derived from snake venom.

Abbreviations

A: *α* angle; A1: The aggregation rates at 1 min; A3: The aggregation rates at 3 min; A5: The aggregation rates at 5 min; ADP: Adenosine diphosphate; AHVPI: *Agkistrodon halys* venom platelet inhibitor; AHVPI-high: The high-dose AHVPI (0.2 mg/kg body weight); AHVPI-low: The low-dose AHVPI (0.05 mg/kg body weight); AHVPI-medium: The medium-dose AHVPI (0.1 mg/kg body weight); AMI: Acute myocardial infarction; ECG: Electrocardiogram; ELISA: Enzyme-linked immunosorbent assay; GPs: Platelet

membrane glycoproteins; GPVI: Platelet membrane glycoprotein VI; HE: Hematoxylin and eosin; IRI: Ischemia-reperfusion injury; *K*: Clot formation time; LAD: Left anterior descending coronary artery; MA: Maximum amplitude; MIRI: Myocardial ischemia-reperfusion injury; *R*: Coagulation time; TEG: Thromboelastography.

Authors' Contributions

Juan Wu, Gui-lin Feng, Wei Li, Xue Zhao, Neng-sheng Bao, Tian-yu Ge, Xi Huang, Qing-quan Xue, and He Zhang: Conceiving and designing the study; Juan Wu, Gui-lin Feng, Qing-quan Xue, and He Zhang: Collecting the data; Juan Wu, Gui-lin Feng, Wei Li, Xue Zhao, Neng-sheng Bao, Tian-yu Ge, and Xi Huang: Analyzing and interpreting the data; Juan Wu, Gui-lin Feng, Qing-quan Xue, and He Zhang: Writing the manuscript; Qing-quan Xue and He Zhang: Providing critical revisions that are important for the intellectual content. All authors approving the final version of the manuscript.

Declaration of Conflicting Interests

The authors declared no potential conflicts of interest with respect to the research, authorship, and/or publication of this article.

Ethical Approval and Informed Consent

This study was conducted in accordance with the Declaration of Helsinki. All animal experiments were reviewed and approved by the Institutional Animal Ethics Committee of Wannan Medical College (IAEC Protocol Approval Number: Wannan Medical College/IAEC/LLSC-2022-267; approval date: January 20, 2022). Written informed consent was not applicable because this was an experiment involving animals alone.

Funding

The authors disclosed receipt of the following financial support for the research, authorship, and/or publication of this article: Key Project of Natural Science in the Universities of Anhui Province (No. 2024AH051949) and Key Project of Natural Science of Wannan Medical College (No. WK2022Z11).

ORCID iD

He Zhang https://orcid.org/0009-0008-6093-7280

References

Aggarwal, P., Rekwal, L., Sinha, S. K., Nath, R. K., Khanra, D., & Singh, A. P. (2021). Predictors of no-reflow phenomenon following percutaneous coronary intervention for ST-segment elevation myocardial infarction. *Annales de Cardiologie et d'Angéiologie*, *70*(3), 136–142. https://doi.org/10.1016/j.ancard.2021.04.004

Alenazy, F. O., & Thomas, M. R. (2021). Novel antiplatelet targets in the treatment of acute coronary syndromes. *Platelets*, *32*(1), 15–28. https://doi.org/10.1080/09537104.2020.1763731

Alpert, J. S. (2023). New coronary heart disease risk factors. *The American Journal of Medicine*, *136*(4), 331–332. https://doi.org/10.1016/j.amjmed.2022.08.002

Borst, O., & Gawaz, M. (2021). Glycoprotein VI—Novel target in antiplatelet medication. *Pharmacology & Therapeutics*, *217*, 107630. https://doi.org/10.1016/j.pharmthera.2020.107630

Caiazzo, G., Musci, R. L., Frediani, L., Umińska, J., Wanha, W., Filipiak, K. J., Kubica, J., & Navarese, E. P. (2020). State of the art: No-reflow phenomenon. *Cardiology Clinics*, *38*(4), 563–573. https://doi.org/10.1016/j.ccl.2020.07.001

Chatterjee, M., Ehrenberg, A., Toska, L. M., Metz, L. M., Klier, M., Krueger, I., Reusswig, F., & Elvers, M. (2020). Molecular drivers of platelet activation: Unraveling novel targets for anti-thrombotic and anti-thrombo-inflammatory therapy. *International Journal of Molecular Sciences*, *21*(21), 7906. https://doi.org/10.3390/ijms21217906

Denorme, F., & Campbell, R. A. (2022). Procoagulant platelets: Novel players in thromboinflammation. *American Journal of Physiology. Cell physiology*, *323*(4), C951–C958. https://doi.org/10.1152/ajpcell.00252.2022

Farmer, D. G., Anselmo, D., Da Shen, X., Ke, B., Carmody, I. C., Gao, F., Lassman, C., McDiarmid, S. V., Shaw, G., Busuttil, R. W., & Kupiec-Weglinski, J. W. (2005). Disruption of P-selectin signaling modulates cell trafficking and results in improved outcomes after mouse warm intestinal ischemia and reperfusion injury. *Transplantation*, *80*(6), 828–835. https://doi.org/10.1097/01.tp.0000174337.53658.b0

Fu, W. W., Yu, X. F., Xue, Y., Yu, P., Wu, X. J., Xu, H. L., & Sui, D. Y. (2019). Establishment and evaluation of rat models of myocardial ischemia reperfusion-related no-reflow under non-artificial ventilator. *Journal of Jilin University (Medicine Edition) , 45*(5), 1058-1062.

Fuentes, E. (2022). Modulation of glycoprotein VI and its downstream signaling pathways as an antiplatelet target. *International Journal of Molecular Sciences*, *23*(17), 9882. https://doi.org/10.3390/ijms23179882

Gawaz, M., Vogel, S., Pfannenberg, C., Pichler, B., Langer, H., & Bigalke, B. (2014). Implications of glycoprotein VI for theranostics. *Thrombosis and Haemostasis*, *112*(1), 26–31. https://doi.org/10.1160/th13-09-0756

Huang, L., Zhang, G. B., Min, Z. X., Ma, K. R., Zheng, R. Q., Sun, Y., & Wu, J. (2012). Effect and mechanism of platelet inhibitor from *Agkistrodon halys* venom on artery thrombosis. *Chinese Journal of Clinical Pharmacology and Therapeutics*, *17*(12), 1355–1360.

Kim, S. C., Boehm, O., Meyer, R., Hoeft, A., Knüfermann, P., & Baumgarten, G. (2012). A murine closed-chest model of myocardial ischemia and reperfusion. *Journal of Visualized Experiments*, (65), e3896. https://doi.org/10.3791/3896

McEver, R. P. (2015). Selectins: Initiators of leucocyte adhesion and signalling at the vascular wall. *Cardiovascular Research*, *107*(3), 331–339. https://doi.org/10.1093/cvr/cvv154

Na, J., Zhang, G. B., Huang, L., Wang, F., Zhang, Y., & Wu, J. (2014). Effects of platelet inhibitor from *Agkistrodon halys* venom on artery thrombosis in rabbit. *Chinese Journal of Clinical Pharmacology and Therapeutics*, *19*(09), 987–990.

Navarro, S., Starke, A., Heemskerk, J. W. M., Kuijpers, M. J. E., Stegner, D., & Nieswandt, B. (2022). Targeting of a conserved epitope in mouse and human GPVI differently affects receptor function. *International Journal of Molecular Sciences*, *23*(15), 8610. https://doi.org/10.3390/ijms23158610

Nieswandt, B., Pleines, I., & Bender, M. (2011). Platelet adhesion and activation mechanisms in arterial thrombosis and ischaemic stroke. *Journal of Thrombosis and Haemostasis*, *9*(Suppl 1), 92–104. https://doi.org/10.1111/j.1538-7836.2011.04361.x

Nuyttens, B. P., Thijs, T., Deckmyn, H., & Broos, K. (2011). Platelet adhesion to collagen. *Thrombosis Research*, *127*(Suppl. 2), S26–S29.

Parodi, G., Marcucci, R., Valenti, R., Gori, A. M., Migliorini, A., Giusti, B., Buonamici, P., Gensini, G. F., Abbate, R., & Antoniucci, D. (2011). High residual platelet reactivity after clopidogrel loading and long-term cardiovascular events among patients with acute coronary syndromes undergoing PCI. *JAMA*, *306*(11), 1215–1223. https://doi.org/10.1001/jama.2011.1332

Sagris, M., Apostolos, A., Theofilis, P., Ktenopoulos, N., Katsaros, O., Tsalamandris, S., Tsioufis, K., Toutouzas, K., & Tousoulis, D. (2024). Myocardial ischemia-reperfusion injury: Unraveling pathophysiology, clinical manifestations, and emerging prevention strategies. *Biomedicines*, *12*(4), 802. https://doi.org/10.3390/biomedicines12040802

Schanze, N., Hamad, M. A., Nührenberg, T. G., Bode, C., & Duerschmied, D. (2023). Platelets in myocardial ischemia/reperfusion injury. *Hamostaseologie*, *43*(2), 110–121. https://doi.org/10.1055/a-1739-9351

Schirone, L., Forte, M., D'Ambrosio, L., Valenti, V., Vecchio, D., Schiavon, S., Spinosa, G., Sarto, G., Petrozza, V., Frati, G., & Sciarretta, S. (2022). An overview of the molecular mechanisms associated with myocardial ischemic injury: State of the art and translational perspectives. *Cells*, *11*(7), 1165. https://doi.org/10.3390/cells11071165

Schlesinger, M. (2018). Role of platelets and platelet receptors in cancer metastasis. *Journal of Hematology & Oncology*, *11*(1), 125. https://doi.org/10.1186/s13045-018-0669-2

Schulz, C., Leuschen, N. V., Fröhlich, T., Lorenz, M., Pfeiler, S., Gleissner, C. A., Kremmer, E., Kessler, M., Khandoga, A. G., Engelmann, B., Ley, K., Massberg, S., & Arnold, G. J. (2010). Identification of novel downstream targets of platelet glycoprotein VI activation by differential proteome analysis: Implications for thrombus formation. *Blood*, *115*(20), 4102–4110. https://doi.org/10.1182/blood-2009-07-230268

Senis, Y. A., Mazharian, A., & Mori, J. (2014). Src family kinases: At the forefront of platelet activation. *Blood*, *124*(13), 2013–2024. https://doi.org/10.1182/blood-2014-01-453134

Slater, A., Khattak, S., & Thomas, M. R. (2024). GPVI inhibition: Advancing antithrombotic therapy in cardiovascular disease. *European Heart Journal. Cardiovascular Pharmacotherapy*, *10*(5), 465–473. https://doi.org/10.1093/ehjcvp/pvae018

Song, Y. M., Tang, X. X., Chen, X. G., Gao, B. B., Gao, E., Bai, L., & Lv, X. R. (2005). Effects of scorpion venom bioactive polypolypeptides on platelet aggregation and thrombosis and plasma 6-keto-PG F1alpha and TXB2 in rabbits and rats. *Toxicon: Official Journal of the International Society on Toxinology*, *46*(2), 230–235. https://doi.org/10.1016/j.toxicon.2005.04.012

Stewart, R. A. H., Held, C., Krug-Gourley, S., Waterworth, D., Stebbins, A., Chiswell, K., Hagstrom, E., Armstrong, P. W., Wallentin, L., & White, H. (2019). Cardiovascular and lifestyle risk factors and cognitive function in patients with stable coronary heart disease. *Journal of the American Heart Association*, *8*(7), e010641. https://doi.org/10.1161/jaha.118.010641

Stoll, G., Nieswandt, B., & Schuhmann, M. K. (2024). Ischemia/reperfusion injury in acute human and experimental stroke: Focus on thrombo-inflammatory mechanisms and treatments. *Neurological Research and Practice*, *6*(1), 57. https://doi.org/10.1186/s42466-024-00355-y

Tong, H. Q., Fan, M. L., Sun, T., Zhang, H. W., Han, J., Wang, M. X., Chen, J. D., Sun, W. X., Chen, X. H., & Wu, M. H. (2022). Improved rodent model of myocardial ischemia and reperfusion injury. *Journal of Visualized Experiments: JoVE*, (181). https://doi.org/10.3791/63510

Veninga, A., Handtke, S., Aurich, K., Tullemans, B. M. E., Brouns, S. L. N., Schwarz, S. L., Heubel-Moenen, F. C. J. I., Greinacher, A., Heemskerk, J. W. M., van der Meijden, P. E. J., & Thiele, T. (2022). GPVI expression is linked to platelet size, age, and reactivity. *Blood Advances*, *6*(14), 4162–4173. https://doi.org/10.1182/bloodadvances.2021006904

Wang, J., Liu, Y., Liu, Y., Huang, H., Roy, S., Song, Z., & Guo, B. (2023). Recent advances in nanomedicines for imaging and therapy of myocardial ischemia-reperfusion injury. *Journal of Controlled Release*, *353*, 563–590. https://doi.org/10.1016/j.jconrel.2022.11.057

Wang, L., Liu, Y., Tian, R., Zuo, W., Qian, H., Wang, L., Yang, X., Liu, Z., & Zhang, S. (2023). What do we know about platelets in myocardial ischemia-reperfusion injury and why is it important? *Thrombosis Research*, *229*, 114–126. https://doi.org/10.1016/j.thromres.2023.06.022

Whitton, T. P., & Healy, W. J. (2023). Review of thromboelastography (TEG): Medical and surgical applications. *Therapeutic Advances in Pulmonary and Critical Care Medicine*, *18*, 29768675231208426. https://doi.org/10.1177/29768675231208426

Xing, Y., Sui, Z., Liu, Y., Wang, M. M., Wei, X., Lu, Q., Chen, R., Wu, M., Wang, Y., Zhao, Y. H., Guo, F., Cao, J. L., Qi, J., & Wang, W. (2022). Blunting TRPML1 channels protects myocardial ischemia/reperfusion injury by restoring impaired cardiomyocyte autophagy. *Basic Research in Cardiology*, *117*(1), 20. https://doi.org/10.1007/s00395-022-00930-x

Yang, M., Huo, X., Miao, Z., & Wang, Y. (2019). Platelet glycoprotein IIb/IIIa receptor inhibitor tirofiban in acute ischemic stroke. *Drugs*, *79*(5), 515–529. https://doi.org/10.1007/s40265-019-01078-0

Zahid, M., Loyau, S., Bouabdelli, M., Aubrey, N., Jandrot-Perrus, M., & Billiald, P. (2011). Design and reshaping of an scFv directed against human platelet glycoprotein VI with diagnostic potential. *Analytical Biochemistry*, *417*(2), 274–282. https://doi.org/10.1016/j.ab.2011.06.036